

PLASMA POTENTIAL EVOLUTION IN VARIOUS OPERATIONAL MODES IN THE TUMAN-3M TOKAMAK

L.G. Askinazi¹, V.A. Kornev¹, S.V. Krikunov¹, L.I. Krupnik², S.V. Lebedev¹,

A.I. Smirnov¹, M.Tendler³, A.S.Tukachinsky¹, M.I. Vildjunas¹, N.A. Zhubr¹

¹*Ioffe Institute, 194021 St.Petersburg, Russia*

²*IPP, Kharkov Institute of Physics and Technology, 61108 Kharkov, Ukraine*

³*Alfven Lab., Euratom NFR Association, Royal Institute of Technology, Stockholm, Sweden*

Introduction

Spatial structure and temporal dynamics of the plasma potential in the small tokamak TUMAN-3M ($R=0.55\text{m}$, $a=0.22\text{m}$, $I_p^{\text{max}}=0.16\text{MA}$, $B_{\text{tor}}^{\text{max}}=0.8\text{T}$, $n_e < 5 \times 10^{19}\text{cm}^{-3}$, $T_e < 500\text{eV}$, $T_i < 200\text{eV}$, $q_{\text{lim}} \sim 2.3-2.6$) was studied in different modes of plasma heating and confinement, namely, in the ohmic L- and H-modes and NBI, with and without low frequency MHD oscillations. Central plasma potential was measured by heavy ion beam probe (HIBP) [1].

Plasma potential evolution in Counter-NBI heated plasma

Central plasma potential studies were carried out in a scenario with ohmic L-H transition followed (with a delay of $\sim 10\text{ms}$) by Counter-NBI heating pulse. The NBI

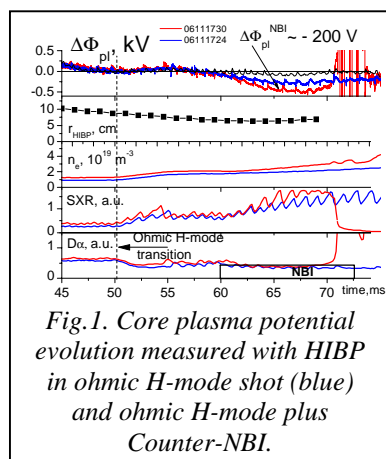


Fig.1. Core plasma potential evolution measured with HIBP in ohmic H-mode shot (blue) and ohmic H-mode plus Counter-NBI.

application on the TUMAN-3M is discussed in [2] in more detail. Measurements of the electric potential were performed by probing the core plasma with 80 keV K^+ ions. Upper box of the Fig. 1 displays the plasma potential evolution measured with HIBP in two shots: #06111730, ohmic H-mode +Counter-NBI (red lines) and #06111724, ohmic H-mode only (blue lines). For a comparison, the potential evolution measured in ohmic L-mode shot is also displayed in the same box (black line). It is clearly seen that potential tends to be more negative after the L-H transition, though it

changes rather slowly during $\sim 8\text{ms}$ after the transition. The location of the point of potential measurement (shown by black squares in a separate box in the same Figure) was nearby $r=6-8\text{cm}$, $r/a=0.25-0.33$, that is well inside the edge transport barrier located near $r=20\text{cm}$. A slow drift of the sample volume is caused by $B_T \neq \text{const}(t)$. A relatively slow evolution of the central potential corresponds to a gradual change in plasma density profile after the edge

transport barrier formation. After the start of NBI heating, central plasma potential gradually becomes even more negative (for $\sim 200V$) than it was in ohmic-H-mode phase. This effect may be a result of orbit losses of fast ions created due to the Counter-NBI, with some additional effect of toroidal momentum and plasma pressure input from the injection.

Positive perturbation of plasma potential during MHD bursts

Earlier, a positive peripheral radial electric field perturbation created by a rotating MHD island has been measured on the TUMAN-3M using Langmuire probes [3] and reflectometry [4]. The MHD event under consideration developed routinely in the first plasma current ramp up stage, with non-stationary current profile, and revealed itself on Mirnov coil signals as a burst ($\sim 7-8ms$ long) of low frequency, low m , n oscillations. From analysis of Mirnov coil array signals and multi-channel microwave interferometer data it was concluded that the MHD perturbation had the island structure, with location near $r=17-19$ cm and half-width of 1.5-2 cm (see [5] for details of the procedure). In this study the HIBP was used for the central potential evolution measurement during the MHD burst. The initial location of the sample volume was at $r=12$ cm, changing slowly to $r=10$ cm due to the B_T non-constancy. Hence, the point of potential measurement was located well inside the chain of the magnetic islands. It was observed, that core plasma potential had exhibited strong positive perturbation up to 700V correlated with the MHD burst, Fig. 2. If such a burst of MHD oscillations was excited in the H-mode stage of the discharge, the accompanying positive electric potential (and radial electric field) was able to cause the H-mode termination - probably, because of “natural” negative H-mode radial electric field being overcome by the perturbation. An example of such behavior is shown in Fig.3. In this case the MHD burst took place at the beginning of the NBI heating pulse, and led to $\sim 700V$ positive perturbation of plasma potential, which was accompanied by the H-L transition. The most probable mechanism of the positive field build-up near the external boundary of the chain of the islands during MHD burst is thought to be a loss of fast electrons along partly disturbed magnetic field lines [3]. As it is found in this work, the electric field perturbation caused by the island is not located in the edge solely, but reaches to the plasma center. The

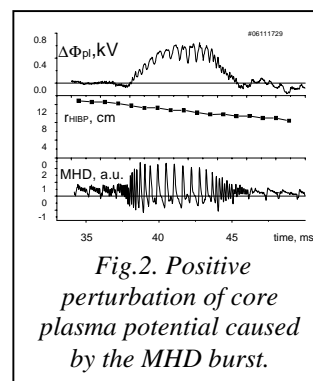


Fig.2. Positive perturbation of core plasma potential caused by the MHD burst.

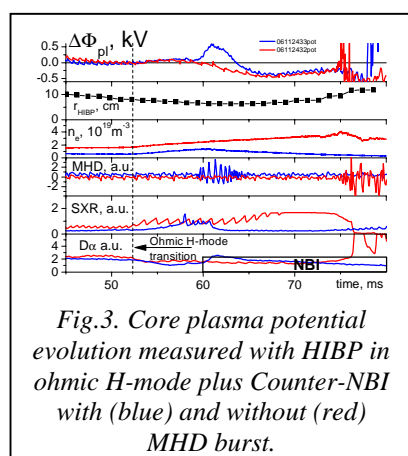


Fig.3. Core plasma potential evolution measured with HIBP in ohmic H-mode plus Counter-NBI with (blue) and without (red) MHD burst.

Fig.3. In this case the MHD burst took place at the beginning of the NBI heating pulse, and led to $\sim 700V$ positive perturbation of plasma potential, which was accompanied by the H-L transition. The most probable mechanism of the positive field build-up near the external boundary of the chain of the islands during MHD burst is thought to be a loss of fast electrons along partly disturbed magnetic field lines [3]. As it is found in this work, the electric field perturbation caused by the island is not located in the edge solely, but reaches to the plasma center. The

mechanism of radial electric field generation by the MHD island is addressed quantitatively in [7].

Observation of Geodesic Acoustic Mode in core plasma

Another interesting phenomenon observed with the HIBP on the TUMAN-3M is quasi-coherent oscillations of plasma potential. These oscillations exist in the TUMAN-3M plasma at the initial stage of the discharge, while the current profile is not stable, usually disappearing after $j(r)$ becomes stationary, but sometimes surviving to the end of the shot. These oscillations has frequency around $\sim 30\text{kHz}$ and relative amplitude up to $\delta\phi/\phi \sim 0.3$. At the same time, local density signal (which is simply proportional to the intensity of the secondary beam of the HIBP) does not exhibit noticeable oscillations ($\delta n/n \leq 0.05$). No oscillations near that frequency were seen on any other diagnostic signals, such as Mirnov coils, interferometer and SXR chords. For example, spectral range of low frequency MHD oscillations in the TUMAN-3M have higher boundary of approximately 12-13 kHz. The frequency of the potential oscillations is close to the geodesic acoustic mode scaling (GAM) $f_{\text{GAM}} \sim 1/(2\pi R)(2T_e/m_i)^{1/2} \sim 30\text{kHz}$, provided that $T_e \sim 100\text{eV}$. Another feature, namely $\delta\phi/\phi \gg \delta n/n$ is also typical for the GAM, especially when observed in equatorial plane [8].

In the GAM studies, the sample volume was located in a region $r \sim 8\text{cm}$, that corresponds to $r/a \sim 0.33$, according to numerical calculations of probing beam trajectories. It is not very usual for GAMs, which, as a rule, are located at the very edge of the plasma column [9]. So, the central location of the GAM in our experiment had to be cross-checked. Independent information on the location of the GAM in the TUMAN-3M was obtained in a shot with strong saw-tooth oscillations co-existing with GAMs, Fig.4. In this shot, the GAMs were clearly seen in HIBP potential signal, while the saw-teeth were simultaneously registered by HIBP density channel and by the multi-chord microwave interferometer.

Analyzing phase relations between the HIBP density channel and interferometer chord signals, it was found that the HIBP sample volume resided somewhere in a region $r < 8\text{cm}$. So, the GAM location around $r \sim 8\text{cm}$ found from the calculation of the HIBP

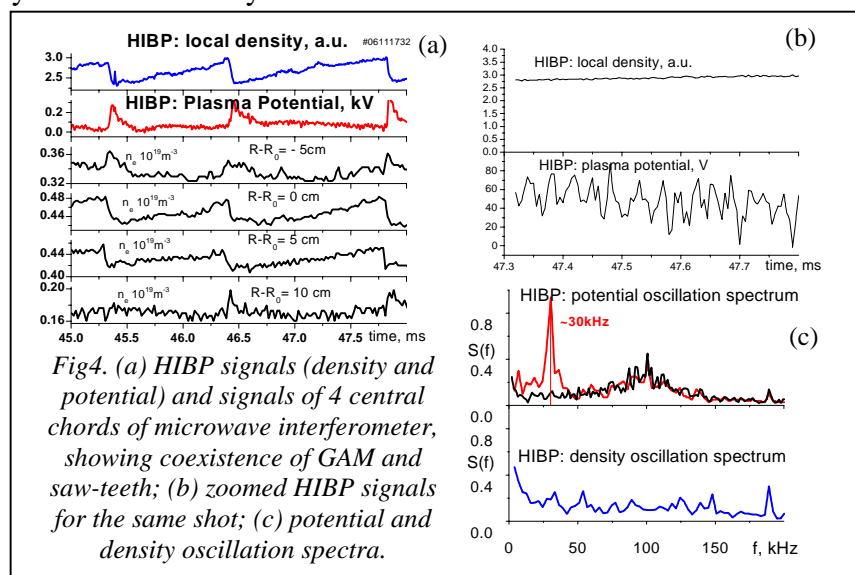


Fig.4. (a) HIBP signals (density and potential) and signals of 4 central chords of microwave interferometer, showing coexistence of GAM and saw-teeth; (b) zoomed HIBP signals for the same shot; (c) potential and density oscillation spectra.

trajectories does not look very unbelievable.

Another interesting observation about this shot is strong ($\sim 200\text{V}$) positive perturbation of central plasma potential in tact with saw-tooth crash, clearly seen in Fig.4a. It may be caused by the loss of fast electrons as a result of the crash, in a way similar to that discussed above for the MHD island.

Summary

In a scenario with Counter-NBI it was found using HIBP that, due to the NBI effect (most probably, orbit loss with some heating and momentum impact), core plasma potential gradually became more negative (for $\sim 200\text{V}$).

Strong positive perturbation of the core plasma potential was registered by the HIBP during the burst of peripheral MHDs with low m , n . If such a burst takes place in the H-mode (both ohmic and counter-NBI heated), the positive potential perturbation leads to H-mode termination. The most probable mechanism of the positive field build-up during MHD burst is though to be a loss of fast electrons along partly disturbed magnetic field lines near the island's separatrix [3,4]. This mechanism is similar to the ergodic divertor's action on the TEXTOR [6], where radial electric field modification by the electron losses was also discussed. A quantitative analysis of the subject may be found in [7]. Similar mechanism may be responsible for a positive perturbation of central plasma potential registered in the saw-tooth crashes.

The GAM with $\delta\phi/\phi \sim 0.3$ and $\delta\phi/\phi \gg \delta n/n \sim 0.05$ where observed with HIBP in a core region of the TUMAN-3M $r/a \sim 0.33$ in the current ramp phase. Further studies are needed to reveal a possible connection between the GAM evolution and plasma confinement in the TUMAN-3M.

Acknowledgment

This work was supported by RFBR grants 07-02-00276, 05-02-17810 and 06-02-16785 and Grant of President of Russian Federation NSH-5149.2006.2.

References

1. L. G. Askinazi, V. A. Kornev, S. V. Lebedev et al, Rev. Sci. Inst., **75**, 3517-1519 (2004)
2. S.V. Lebedev, L.G. Askinazi, A.G. Barsukov et al, Proc. 21st IAEA Fusion Energy Conference, Chengdu, China, 16-21 October 2006, EX/P3-15
3. L G Askinazi, V E Golant, V A Kornev et al, Plasma Phys. Control. Fusion, **48**, A85-A91 (2006)
4. V.V. Bulanin, L.G. Askinazi, S.V. Lebedev et al, Plasma Phys. Contr. Fusion, **48** A101-A107, (2006)
5. V.A.Kornev, L.G.Askinazi, M.I.Vil'dzhyunas et al, Plasma Physics Reports, **31**, 803-808 (2005)
6. K. H. Finken, S. S. Abdullaev, M. W. Jakubowski et al, Phys. Rev. Lett. **98**, 065001(4) (2007)
7. V.V. Rozhansky, M. Tendler, and E.Kaveeva, this conference
8. A.V. Melnikov, V.A. Vershkov, L.G. Eliseev et al, Plasma Phys. Control. Fusion **48** S87-S110 (2006)
9. T. Ido, Y Miura, K Kamiya et al., Plasma Phys. Control. Fusion **48** S41 (2006).